

Dielectric Study on Molecular Motions of Poly(glutamic acid) in Aqueous Solution over a Frequency Range of 10^5 – 10^{10} Hz

Satoru Mashimo,* Nobuhiro Miura, Naoki Shinyashiki, and Tsuneo Ota

Department of Physics, Tokai University, Hiratuka-shi, Kanagawa 259-12, Japan

Received June 18, 1993; Revised Manuscript Received September 14, 1993*

ABSTRACT: Dielectric relaxation measurements over an extremely wide frequency region from 100 kHz to 20 GHz were performed on poly(glutamic acid) in dilute aqueous solution at 25 °C. Three relaxation peaks could be found. The high frequency peak around 10 GHz could be easily due to orientation of water molecules, and the intermediate one around 100 MHz could be assigned to a micro-Brownian motion of the main chain. The relaxation strength of the intermediate process is proportional to $f_c^{4.9}$, where f_c is the fraction of coil. This means that linear linkage of five repeat units in the coiled part is required for the motion. At the limit of $f_c = 1$, the relaxation time for the lowest frequency process is 1×10^{-8} s, which is in complete agreement with that for the overall rotation of a coiled polymer in solution. On the other hand it takes a value of 5×10^{-6} s at $f_c = 0$, which is reasonably in good agreement with that observed for the overall rotation of a rodlike polymer with the same size in solution.

Introduction

Poly(glutamic acid) (PGA) is one of the good analogues to investigate molecular dynamics of real proteins. It exhibits a helix-coil transition in aqueous solution around pH = 5. If the pH value is less than 5, it prefers the helix structure.¹ The transition could be seen in dielectric properties of the solution too.²⁻⁵ It was reported that the solution shows two relaxation peaks.^{4,5} One observed at around 20 GHz could be concluded to be due to the orientation of water molecules, and the other observed at around 100 MHz was suggested to be caused by the micro-Brownian motion of the polymer chain, judging from the dependence of relaxation strength on the fraction of coiled part.⁴

The repeat unit of PGA has two dipole components: one is perpendicular to the chain contour and the other is parallel to it.^{6,7} Dielectric relaxation due to the former component reflects the micro-Brownian motion of the chain, and that due to the latter reflects the overall rotation of the polymer. The peak of the former relaxation is usually located at a frequency around 100 MHz.^{8,9} If PGA takes a helix structure, hydrogen bonds between oxygen and proton atoms bring a fairly big resultant dipole moment as a whole.¹⁰ Therefore dielectric relaxation strength and relaxation time depend on the molecular weight of the protein. If PGA takes a randomly coiled structure, the relaxation caused by the parallel component has a smaller relaxation strength and a shorter relaxation time than those for the helix structure.

The relaxation peak around 100 MHz was first observed by the use of a time domain reflectometry (TDR) method.⁴ After this observation it was suggested that the peak has a strong possibility of being due to truncation error of the Fourier transform or due to evaluation of the dc conductivity of the electrolyte solution.¹¹ It was further pointed out that only a peak can be seen if the TDR method is employed. However a high frequency impedance measurement on a PGA solution has exhibited clearly the existence of the relaxation peak between 10 and 100 MHz.⁵

Once it was thought that the TDR method is inadequate to measure dielectric material with high dc conductivity like an electrolyte solution. It was believed almost

impossible to evaluate the contribution of the dc conductivity to the complex permittivity, especially in the low frequency region. However it was shown recently that if a standard sample with known permittivity and dc conductivity is employed as a reference and its dc conductivity is adjusted to be nearly the same as that of the unknown sample, the complex permittivity of the unknown sample can be obtained as a function of the ratio of Fourier transforms of the two reflected waves from the known and the unknown samples.¹²⁻¹⁴

In this work we employed this reference TDR method in order to investigate the dielectric properties of PGA in aqueous solutions with various pH values in the frequency range 10^5 – 10^{10} Hz. Our peculiar interest is focused on whether the 100-MHz peak exists or not and on its origin. Around 100 MHz, bound water exhibits certainly a relaxation peak. This was observed already for tropocollagen¹⁵ and DNA.¹⁴ Another origin is the chain motion of the polymer concerned. If so, relaxation strength and relaxation time depend on the fraction of coiled part and the strength should disappear for the helical polymer.

Previous dielectric measurements on the PGA aqueous solution by TDR covered only a narrow frequency range from 50 MHz to 10 GHz according to the time windows used.⁴ Therefore only two relaxation peaks could be observed at around 100 MHz and 10 GHz, respectively. However in this work several time windows including one extremely long time range were employed for the TDR measurements and one more peak could be found at lower frequency.

Experimental Section

The sample preparation was the same as reported in the previous paper.⁴ The PGA sample used in this work is the same as that used in the previous work, which was purchased from Sigma Chemical Co. The viscosity-average molecular weight is 5.1×10^4 . Deionized and distilled water is obtained from Whittaker Bioproduct Inc. The pH value of the solution is varied by adding HCl or NaOH. The concentration of PGA is 5 mg/cm³ for all the solutions measured, and the temperature employed is 25 °C.

The system and the apparatus of TDR measurement were reported already.¹²⁻¹⁴ The measurement procedure is essentially the same as that used previously. If a known sample with known permittivity ϵ_s^* is used as a reference sample, the unknown

* Abstract published in *Advance ACS Abstracts*, November 1, 1993.

permittivity ϵ_X^* is given as

$$\epsilon_X^*(\omega) = \epsilon_S^*(\omega) \frac{1 + \{cf_S/[j\omega(\gamma d)\epsilon_S^*(\omega)]\}\rho f_X}{1 + \{[j\omega(\gamma d)\epsilon_S^*(\omega)]/(cf_S)\}\rho f_S} \quad (1)$$

where

$$\rho = \frac{r_S - r_X}{r_S + r_X}$$

$$f_X = Z_X \cot Z_X \quad Z_X = (\omega d/c)\epsilon_X^*(\omega)^{1/2}$$

$$f_S = Z_S \cot Z_S \quad Z_S = (\omega d/c)\epsilon_S^*(\omega)^{1/2}$$

where $r_X(\omega)$ is the Fourier transform of the reflected wave from the unknown sample, $r_S(\omega)$ is that from the known sample, γd is an electric length of the cell, d is the geometric cell length, c is the speed of propagation, and ω is the angular frequency. When the unknown sample has a dc conductivity σ_X , the known sample is adjusted to have nearly the same conductivity so that $R_S(t) - R_X(t)$ reaches zero or nearly zero at a sufficiently long time. If the adjustment can be done successfully, truncation error for the Fourier transform of $R_S(t) - R_X(t)$ can be avoided. For the measurements of an aqueous solution, water is usually employed as the reference sample and the dc conductivity is adjusted by adding HCl or NaCl, the value of which is determined from the value of $R_S(t)$ at a sufficiently long time where $R_S(t) - R_X(t)$ takes a constant value close to zero. Thus ϵ^* can be determined accurately from eq 1 without the truncation error. Furthermore σ_X can be determined from a plot of ϵ'' against $\log f$ in a very low frequency region. Finally, we obtain $\epsilon^* = \epsilon^* - \sigma_X$ properly.

Two cells with different d and γd were employed in this work. For the accurate measurements in a frequency range higher than 100 MHz, the short cell with $d = 0.01$ mm and $\gamma d = 0.11$ mm is used, and in a range below 1 GHz a long cell with $d = 2.1$ mm and $\gamma d = 4.3$ mm is used. Time windows employed are 5, 20, 50, and 100 ns for the short cell and 200 ns, 500 ns, 1 μ s, and 10 μ s for the long cell. In the overlapping area of frequency between 100 MHz and 1 GHz, data obtained by two different cells are in complete agreement with each other.

Results

The dielectric absorption curve for the sample with pH = 6.77 shows definitely three relaxation peaks, as is seen in Figure 1. If the relaxation process is assumed to be a sum of the three independent processes

$$\epsilon^* = \epsilon_\infty + \sum_{i=1}^3 \frac{\Delta\epsilon_i}{[1 + (j\omega\tau_i)^{\beta_i}]^{\alpha_i}} \quad (2)$$

the complex permittivity ϵ^* can be explained sufficiently, as Figure 1 shows, where ϵ_∞ is the permittivity at the limiting angular frequency $\omega \rightarrow 0$, τ_i is the relaxation time for each process, $\Delta\epsilon_i$ is the relaxation strength, and α_i and β_i are parameters describing a distribution of relaxation times, respectively.¹⁶ For the sample with a pH value >6.45, three relaxation peaks could be observed clearly.

On the other hand for the samples with the pH value between 5.15 and 6.15, the low frequency process l is so big that the process cannot be explained by a sum of two process l and h. At least three processes are required, it is assumed, to explain the total dispersion and absorption curves observed, as Figure 2 shows. A least fitting procedure gives the most appropriate value to each parameter in eq 2. The values thus obtained are listed in Table I. In order to avoid complexity, we use a suffix h for the high frequency process, m for the intermediate process, and l for the low frequency process, respectively. In the previous work,⁴ the process l could be found because of a low resolution in a low frequency region lower than 10 MHz. The process l could not be distinguished from

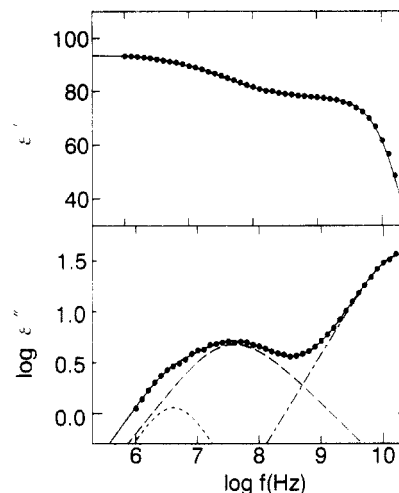


Figure 1. Frequency dependence of the dielectric dispersion and absorption for a PGA aqueous solution (5 mg/cm³, pH = 6.8) at 25 °C. The solid curves are calculated by eq 1. Three relaxation peaks can be seen definitely for the absorption curve at about 4 MHz, 30 MHz, and 18 GHz, respectively.

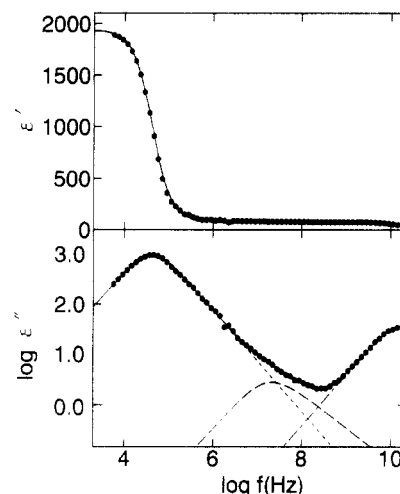


Figure 2. Frequency dependence of the dielectric dispersion and absorption for a PGA aqueous solution (5 mg/cm³, pH = 5.4) at 25 °C. The solid curves are calculated by eq 1. Three relaxation peaks can be seen for the absorption curve.

Table I. Dielectric Relaxation Parameters in Eq 1 Determined for a PGA Aqueous Solution (5 mg/cm³) with Various pH Values at 25 °C

pH	f_c	$\Delta\epsilon_h$	$\log \tau_h$ (s)	α_m	β_m	$\Delta\epsilon_m$	$\log \tau_m$ (s)	α_l	$\Delta\epsilon_l$	$\log \tau_l$ (s)
8.40	0.978	73.0	-11.07	0.82	0.86	15.8	-8.44	1.00	2.5	-7.53
7.20	0.970	72.5	-11.07	0.81	0.86	15.2	-8.40	1.00	3.3	-7.24
6.77	0.967	72.2	-11.07	0.76	0.82	14.5	-8.28	1.00	2.2	-7.41
6.45	0.964	72.6	-11.07	0.77	0.81	14.0	-8.13	1.00	5.3	-6.94
6.15	0.956	72.4	-11.07	0.75	0.78	13.7	-8.14	1.00	47.4	-6.24
5.85	0.926	72.9	-11.07	0.77	0.76	12.2	-8.03	1.00	29.1	-6.29
5.65	0.885	72.6	-11.07	0.76	0.79	9.8	-7.94	1.00	83.2	-6.26
5.40	0.781	73.2	-11.07	0.81	0.96	7.1	-8.01	1.00	1850	-5.41
5.15	0.607	72.2	-11.06	1.00	1.00	2.6	-7.97	0.92	1760	-5.18
4.75	0.342	73.1	-11.06					0.95	5760	-5.29
4.50	0.175	70.8	-11.07					0.94	6730	-5.29

the dc conductivity. Therefore experimental values of the parameters for the process m were fairly different from the values reported previously. Especially there were found large discrepancies for a pH value <5.

The relaxation time τ_m and the relaxation strength $\Delta\epsilon_m$ for the intermediate process are plotted against the pH value in Figure 3. An abrupt change is seen in $\Delta\epsilon_m$ at pH ~ 5.5, where τ_m has the minimum value. In the case of

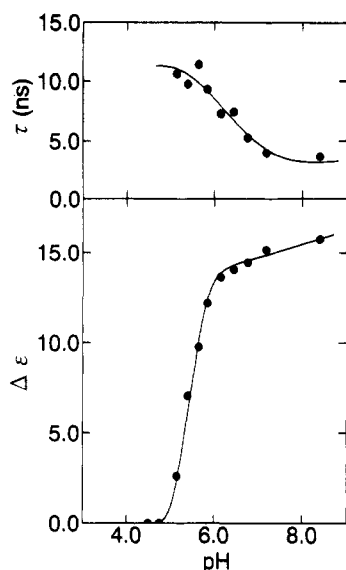


Figure 3. Variation of $\Delta\epsilon_m$ and τ_m with the pH value for a PGA aqueous solution (5 mg/cm³) at 25 °C.

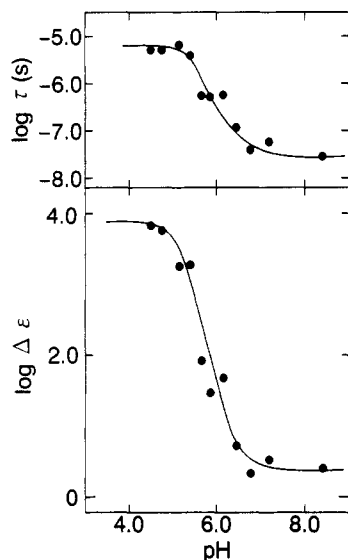


Figure 4. Variation of $\Delta\epsilon_l$ and τ_l with the pH value for a PGA aqueous solution (5 mg/cm³) at 25 °C.

the low frequency process, $\Delta\epsilon_l$ changes little with the pH value if the value is greater than 6.5 but steeply changes in the vicinity of pH = 5.5. Similarly, τ_l changes with the pH value, as Figure 4 shows.

In the case of the high frequency process, both τ_h and $\Delta\epsilon_h$ do not change with the pH value at all. The process can be due to the bulk water process, judging from the relaxation time and relaxation strength. The parameter α_h remains unity for all solutions measured, and β_h is slightly lower but very close to unity.

Discussion

It is known that the PGA shows a helix-coil transition in aqueous solution in a region $4 < \text{pH} < 6$.¹ The present dielectric data on $\Delta\epsilon_m$ and τ_m also exhibit a transition in the same region. In the previous paper we reported the result of molar ellipticity measurements obtained by CD spectra for the same PGA and a fraction of the coiled part.⁴ Therefore present dielectric properties can be plotted against the fraction f_c . In Figure 5 plots of $\Delta\epsilon_m$ and τ_m against f_c are shown, and those of $\Delta\epsilon_l$ and τ_l are shown in Figure 6.

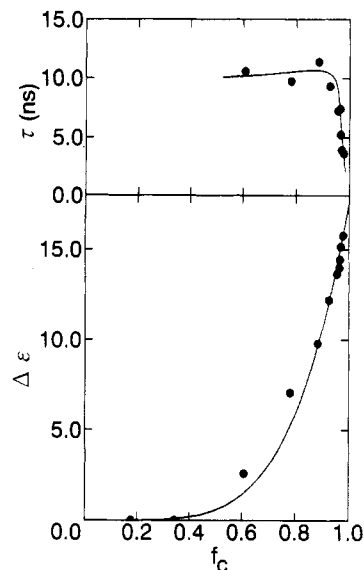


Figure 5. Dependence of τ_m and $\Delta\epsilon_m$ on the fraction of coiled part in a PGA aqueous solution at 25 °C. The solid curve for $\Delta\epsilon_m$ is calculated by eq 17.

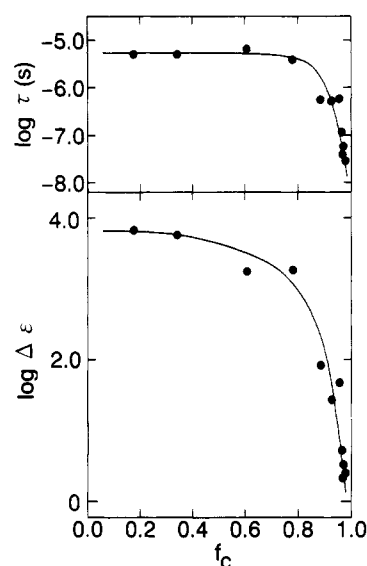


Figure 6. Dependence of $\log \tau_l$ and $\log \Delta\epsilon_l$ on the fraction of coiled part in a PGA aqueous solution at 25 °C.

The total dipole moment of the PGA with degree of polymerization \bar{M} is written as

$$\bar{M} = \sum_{i=1}^n \vec{\mu}_{\perp i} + \sum_{i=1}^n \vec{\mu}_{\parallel i} \quad (3)$$

where $\vec{\mu}_{\perp i}$ is the dipole component of i th repeat unit perpendicular to the chain contour and $\vec{\mu}_{\parallel i}$ is that parallel to the contour. The time-dependent correlation function is given by

$$\langle \bar{M}(0)\bar{M}(t) \rangle = \left\langle \sum_{i=1}^n \vec{\mu}_{\perp i}(0) \sum_{j=1}^n \vec{\mu}_{\perp j}(t) + \sum_{i=1}^n \vec{\mu}_{\parallel i}(0) \sum_{j=1}^n \vec{\mu}_{\parallel j}(t) \right\rangle \quad (4)$$

In general the perpendicular component does not correlate with the parallel one. The former brings about a dielectric relaxation independent of the molecular weight of the polymer⁶ and the latter causes a relaxation depending on it.¹⁰ Therefore the term $\langle \sum_{i=1}^n \vec{\mu}_{\perp i}(0) \sum_{j=1}^n \vec{\mu}_{\parallel j}(t) \rangle$ can be eliminated in eq 3. The first term in eq 4 is rewritten as

$$\begin{aligned} \langle \sum_{i=1}^n \vec{\mu}_{\perp i}(0) \sum_{l=1}^n \vec{\mu}_{\perp l}(t) \rangle &= \mu_{\perp}^2 \left[\sum_{i=1}^n \psi_{\perp i}(t) + \sum_{i \neq l}^n \psi_{\perp il}(t) \right] \\ &= n\mu_{\perp}^2 g(t) \end{aligned} \quad (5)$$

where $\psi_i(t) = \langle \vec{\mu}_{\perp i}(0) \vec{\mu}_{\perp i}(t) \rangle / \mu_{\perp}^2$ is the autocorrelation function of the i th component, $\psi_{il}(t) = \langle \vec{\mu}_{\perp i}(0) \vec{\mu}_{\perp l}(t) \rangle / \mu_{\perp}^2$ is the cross-correlation function between the i th and l th components, and μ_{\perp} is the magnitude of $\vec{\mu}_i$. The function $g(t)$ at $t = 0$ gives the Kirkwood g factor, which usually takes a value between 0.4 and 0.9 for randomly coiled polymers. Orientation of the i th perpendicular component requires a conformational change of neighboring repeat units.¹⁷ In other words, the orientation of the i th component possibly occurs only when a linkage of the neighboring several repeat units forms the coiled part. If it is assumed that the orientation requires the linkage of more than m units, the correlation of the perpendicular components for partially coiled polymer is given by

$$\langle \sum_{i=1}^n \vec{\mu}_{\perp i}(0) \sum_{l=1}^n \vec{\mu}_{\perp l}(t) \rangle = n f_c^s \mu_{\perp}^2 g_s(t; f_c) \quad (6)$$

since the probability of the linkage of s repeat units in the coiled part is given by f_c^s . If $g_s(0; f_c)$ is assumed to be the same as $g(0)$ in eq 5 and $\phi_{\perp}(t; f_c)$ is defined as

$$\phi_{\perp}(t; f_c) = g_s(t; f_c) / g(0) \quad (7)$$

eq 5 is rewritten as

$$\langle \sum_{i=1}^n \vec{\mu}_{\perp i}(0) \sum_{l=1}^n \vec{\mu}_{\perp l}(t) \rangle = (n\mu_{\perp}^2 g(0)) f_c^s \phi_{\perp}(t; f_c) \quad (8)$$

where $\phi_{\perp}(0; f_c) = 1$.

On the other hand, the orientation of $\vec{\mu}_{\parallel i}$ reflects the overall rotation of the polymer molecule, since $\sum_{i=1}^n \vec{\mu}_{\parallel i}$ is proportional to the end-to-end distance of the molecule.¹⁰ Therefore if the polymer is completely random, the dipole correlation is given by

$$\langle \sum_{i=1}^n \vec{\mu}_{\parallel i}(0) \sum_{l=1}^n \vec{\mu}_{\parallel l}(t) \rangle = n\mu_{\parallel}^2 \phi_{\parallel}(t) \quad (9)$$

In the case where the excluded volume effect cannot be ignored eq 9 is written as

$$\langle \sum_{i=1}^n \vec{\mu}_{\parallel i}(0) \sum_{l=1}^n \vec{\mu}_{\parallel l}(t) \rangle = n\mu_{\parallel}^2 h(n) \phi_{\parallel}(t; n) \quad (10)$$

where $h(n)$ depends slightly on n if n is not big enough. If the polymer is a rodlike polymer, we get

$$\langle \sum_{i=1}^n \vec{\mu}_{\parallel i}(0) \sum_{l=1}^n \vec{\mu}_{\parallel l}(t) \rangle = n\mu_{\parallel}^2 (n \cos^2 \theta) \phi_{\parallel}(t; n) \quad (11)$$

where θ is the angle between the helical axis and the parallel component of each dipole. In the case of PGA, it changes from the randomly coiled polymer at $f_c = 1$ to the rodlike polymer at $f_c = 0$, and its fraction of the coiled part changes accordingly with the pH value. Therefore we get the following equation as a total equation for the time correlation:

$$\langle \sum_{i=1}^n \vec{\mu}_{\parallel i}(0) \sum_{l=1}^n \vec{\mu}_{\parallel l}(t) \rangle = n\mu_{\parallel}^2 h(n, f_c) \phi_{\parallel}(t; n, f_c) \quad (12)$$

for PGA, where $h(n, f_c)$ coincides with $h(n)$ if PGA is coiled and it coincides with $n \cos^2 \theta$ if PGA is a helix. In this

work the same polymer is used for all the measurements, then we have

$$\langle \sum_{i=1}^n \vec{\mu}_{\parallel i}(0) \sum_{l=1}^n \vec{\mu}_{\parallel l}(t) \rangle = n\mu_{\parallel}^2 h(f_c) \phi_{\parallel}(t; f_c) \quad (13)$$

Complex permittivity ϵ^* is related to eqs 4, 8, and 13 as

$$\begin{aligned} \epsilon^* - \epsilon_{\infty} - \frac{\Delta\epsilon_h}{[1 + (j\omega\tau)^{\beta_h}]^{\alpha_h}} = \\ \frac{4\pi N n g(0) \mu_{\perp}^2 f_c^s}{3kT} F_1 \int_0^{\infty} e^{-j\omega t} [-\dot{\phi}_{\perp}(t; f_c)] dt + \\ \frac{4\pi N n \mu_{\parallel}^2 h(f_c)}{3kT} F_2 \int_0^{\infty} e^{-j\omega t} [-\dot{\phi}_{\parallel}(t; f_c)] dt \end{aligned} \quad (14)$$

where N is the number of polymer molecules per unit volume and F_1 or F_2 is a ratio of the internal field to the applied field. The Fourier transform of $-\dot{\phi}(t)$ is described empirically by

$$\int_0^{\infty} e^{-j\omega t} [-\dot{\phi}(t)] dt = \frac{1}{[1 + (j\omega\tau)^{\beta}]^{\alpha}} \quad (15)$$

Therefore eq 14 is rewritten as

$$\begin{aligned} \epsilon^* - \epsilon_{\infty} = \frac{\Delta\epsilon_l}{[1 + (j\omega\tau_l)^{\beta_l}]^{\alpha_l}} + \frac{\Delta\epsilon_m}{[1 + (j\omega\tau_m)^{\beta_m}]^{\alpha_m}} + \\ \frac{\Delta\epsilon_h}{[1 + (j\omega\tau_h)^{\beta_h}]^{\alpha_h}} \end{aligned} \quad (16)$$

where the relaxation process denoted by h is the bulk water process which is not concerned in this work. It is natural that F_1 is taken as a constant for the process m . Then we get

$$\Delta\epsilon_m = \frac{4\pi N n \mu_{\perp}^2 g(0) f_c^s F_1}{3kT} = \Delta\epsilon_m^c f_c^s \quad (17)$$

where $\Delta\epsilon_m^c$ is the relaxation strength at $f_c = 1$. Experimental results on $\Delta\epsilon_m$ can be explained satisfactorily by eq 17 in a region where f_c is bigger than 0.8, as is seen in Figure 5, and we obtain $s = 4.9$ and $\Delta\epsilon_m^c = 17.6$, respectively. The value obtained for s is in good agreement with that obtained previously. It is noted that $\Delta\epsilon_m$ vanishes at $f_c \sim 0.4$. This was not found in the previous work.⁴

The chain motion reflecting orientation of the perpendicular component will be influenced by the helical part neighboring the coiled s repeat units. The relaxation time is naturally bigger for the higher constant of the helix part. The experimental result shown in Figure 5 shows that the relaxation time increases radically with a decrease of f_c for $0.85 < f_c < 1$ and remains constant for $f_c < 0.85$.

In the low frequency process, the relaxation strength and the relaxation time depend largely on f_c , as Figure 6 shows. The relaxation time τ_1 extrapolated to $f_c = 1$ is 1×10^{-8} s and is in good agreement with that for the overall rotation of other coiled polymers with the same molecular weight in solution. On the other hand, it has a value of 5×10^{-6} s, if f_c is extrapolated to zero. This value is in good agreement with that of a helical polymer of the same size in solution. Examples are PBLG^{10,18} and poly(*n*-butyl isocyanate).¹⁹ The relaxation time at $f_c = 0$ is also explained as the overall rotation of the ellipsoidal molecule about the short axis.²⁰

If f_c is decreased, the helical part of the PGA molecules is increased. Accordingly, the molecule expands and the relaxation time becomes long. Nevertheless if the helical part increases to the same extent, the relaxation time will

not be able to be explained by rotation of a spherical molecule or that of a rodlike molecule. The fact that the relaxation time observed for $f_c < 0.6$ is constant but the relaxation strength increases rapidly evidences the complicated structure of PGA.

A ratio of the relaxation strength $\Delta\epsilon_1$ at $f_c = 0$ to that at $f_c = 1$ is 1×10^4 . If $F_1 = F_2$ is assumed, the ratio is given by eqs 10 and 11 as $n[\cos^2 \theta/h(n)] \sim n$ and it is expected to take a value close to $n = 3.5 \times 10^2$ for the present PGA. The observed value of 1×10^4 is fairly big compared to the predicted one. This large difference will come from migration of counterions along the PGA helix. The ion migration will always bring about a big strength.

References and Notes

- (1) Doty, P.; Wada, A.; Yang, J. T.; Blout, E. R. *J. Polym. Sci.* **1957**, *23*, 851.
- (2) Nakamura, H.; Wada, A. *Biopolymers* **1981**, *20*, 2567.
- (3) Muller, G.; Van Der Touw, F.; Zwolle, S.; Mandel, M. *Biophys. Chem.* **1974**, *2*, 242.
- (4) Mashimo, S.; Ota, T.; Shinyashiki, N.; Tanaka, S.; Yagihara, S. *Macromolecules* **1989**, *22*, 1285.
- (5) Bordy, F.; Cametti, C.; Paradossi, G. *Macromolecules* **1992**, *25*, 4206.
- (6) Stockmayer, W. H. *Pure Appl. Chem.* **1967**, *15*, 539.
- (7) Bates, T. W.; Ivan, K. J.; Williams, G. *Trans. Faraday Soc.* **1967**, *63*, 1964.
- (8) Mashimo, S. *Macromolecules* **1976**, *9*, 91.
- (9) Miura, N.; Shinyashiki, N.; Mashimo, S. *J. Chem. Phys.* **1992**, *97*, 8722.
- (10) Wada, A. *J. Chem. Phys.* **1959**, *31*, 495.
- (11) Gestblom, B.; Gestblom, P. *Macromolecules* **1991**, *24*, 5823.
- (12) Cole, R. H.; Mashimo, S.; Winsor, P., IV. *J. Phys. Chem.* **1980**, *84*, 786.
- (13) Mashimo, S.; Umehara, T.; Ota, T.; Kuwabara, S.; Shinyashiki, N.; Yagihara, S. *J. Mol. Liq.* **1987**, *36*, 135.
- (14) Umehara, T.; Kuwabara, S.; Mashimo, S.; Yagihara, S. *Biopolymers* **1990**, *30*, 649.
- (15) Shinyashiki, N.; Asaka, N.; Mashimo, S.; Yagihara, S.; Sasaki, N. *Biopolymers* **1990**, *29*, 1185.
- (16) Havriliak, S.; Negami, S. *Polymer* **1967**, *8*, 161.
- (17) Mashimo, S. *J. Chem. Phys.* **1977**, *67*, 2651.
- (18) Wada, A. *J. Polym. Sci.* **1960**, *45*, 145.
- (19) Yu, H.; Bur, A. J.; Fetters, L. J. *J. Chem. Phys.* **1966**, *44*, 2568.
- (20) Perrin, F. *J. Phys. Radium* **1934**, *5*, 497.